Article

Discovery Medicine 2026; 38(208): 1583–1596
https://doi.org/10.24976/Discov.Med.202638208.124

Esketamine Alleviates Limb Ischemia-Reperfusion-Induced Lung Injury by Inducing Macrophage Polarization

Meng Wang[1], Wenjuan Wang[1], Peng Wang[1], Heng Wen[2], Jiawei Cun[3], Qian Ma[1,*]

[1]Department of Anesthesiology, General Hospital of Ningxia Medical University, 750004 Yinchuan, Ningxia, China
[2]Department of Anesthesiology, The First Affiliated Hospital of Zhejiang University School of Medicine, 310006 Hangzhou, Zhejiang, China
[3]Clinical Medicine, Ningxia Medical University, 750004 Yinchuan, Ningxia, China
*Correspondence: maqian@nxmu.edu.cn (Qian Ma)
Submitted: 11 December 2025 Revised: 15 January 2026 Accepted: 4 March 2026 Published: 20 May 2026

Background: Limb ischemia-reperfusion-induced acute lung injury (LIR-ALI) remains without effective therapies, with macrophage polarization playing a pivotal role in its pathology. This study explored the protective effects of esketamine in LIR-ALI, focusing on its modulation of macrophage polarization through the TLR4/NF-κB/NLRP3 pathway.

Methods: Sprague-Dawley rats subjected to LIR (bilateral femoral artery clamping for 2 hours followed by reperfusion) under mechanical ventilation were treated with esketamine (5 mg/kg) or saline. Lung injury, inflammatory cytokines (Enzyme-linked immunosorbent assay, ELISA), and macrophage polarization markers (iNOS, Arg-1) were evaluated. *In vitro*, THP-1 macrophages were pretreated with esketamine (50 µM), stimulated with LIR-ALI rat serum, and co-cultured with BEAS-2B epithelial cells. Macrophage polarization (NOS2, Arg-1, CD86, CD206), epithelial cell viability (CCK-8), inflammatory cytokines, oxidative stress markers (superoxide dismutase (SOD), malondialdehyde (MDA)), and TLR4/NF-κB/NLRP3 pathway proteins were assessed. LPS was used to assess pathway dependency.

Results: Esketamine significantly reduced LIR-induced lung pathological damage and inflammatory cell infiltration in rats. It lowered pro-inflammatory cytokines (IL-1β, IL-6, TNF-α) and elevated IL-10 in bronchoalveolar lavage fluid (BALF) ($p < 0.01$), while promoting M2 macrophage polarization (decreased iNOS, increased Arg-1) in lung tissue ($p < 0.05$). *In vitro*, esketamine redirected LIR-ALI serum-stimulated macrophages toward the M2 phenotype (decreased NOS2/CD86, increased Arg-1/CD206) ($p < 0.001$), enhanced BEAS-2B cell viability, and mitigated inflammation and oxidative stress ($p < 0.01$). These effects were linked to esketamine's inhibition of the TLR4/NF-κB/NLRP3 pathway in macrophages ($p < 0.01$). LPS reversed esketamine's protective effects, including its modulation of macrophage polarization and the signaling pathway ($p < 0.05$).

Conclusion: Esketamine mitigates LIR-ALI by promoting M2 macrophage polarization through the suppression of the TLR4/NF-κB/NLRP3 axis, suggesting its potential as a therapeutic strategy for LIR-ALI.

Keywords: esketamine; limb ischemia-reperfusion; acute lung injury; macrophage polarization; TLR4/NF-κB/NLRP3 axis

Introduction

Limb ischemia-reperfusion (LIR) is a common pathological event in clinical conditions such as trauma and vascular surgery, often resulting in distal organ injury, with acute lung injury (ALI) being particularly prevalent and presenting significant clinical challenges [1]. Limb ischemia-reperfusion-induced acute lung injury (LIR-ALI) is characterized by extensive pulmonary inflammatory cell infiltration, edema, aggravated oxidative stress, thickened alveolar walls, and disruption of the alveolar-capillary barrier, which can progress to severe conditions such as acute respiratory distress syndrome [2]. Epidemiological data show that ALI has a mortality rate of 35%–40% and remains largely refractory to treatment [3]. Current clinical management primarily relies on supportive care, lacking targeted pharmacological treatments addressing the core pathogenic mechanisms of LIR-ALI. Thus, there is an urgent need to develop novel therapeutic strategies based on the underlying pathophysiology to effectively modulate the mechanisms driving LIR-ALI.

Macrophages, as key components of the innate immune system, play a pivotal role in regulating tissue homeostasis, inflammation, and tissue repair [4]. In the pathogenesis of ALI, M1 macrophages exacerbate inflammatory damage through the secretion of pro-inflammatory mediators (Tumor Necrosis Factor-alpha (TNF-α), Interleukin-1 beta (IL-1β)), while M2 macrophages reduce inflammation and promote repair through Interleukin-10 (IL-10) and Arginase-1 (Arg-1) secretion [5,6]. Activation of the NOD-like receptor protein 3 (NLRP3) inflammasome is a critical regulatory point in the inflammatory signaling triggered

by LIR. Experimental evidence shows that inhibiting the NLRP3 inflammasome promotes M2 polarization and alleviates inflammation associated with ALI [7]. Downregulation of NLRP3 reduces LIR-ALI manifestations in rats, including pulmonary edema, tissue damage, and expression of inflammatory factors [8]. However, the exact mechanisms underlying macrophage polarization in LIR-ALI remain incompletely understood.

Toll-like receptor 4 (TLR4), a pattern recognition receptor (PRR), plays a pivotal role in regulating immune responses and inflammation. TLR4 modulates microglial inflammation via the NF-κB pathway [9], and inhibition of TLR4/NF-κB signaling has been shown to reduce cerebral infarction volume and improve brain injury in cerebral ischemia-reperfusion models [10]. Emerging evidence also indicates that the TLR4/NF-κB pathway regulates macrophage polarization in lung injury. Pharmacological inhibition of TLR4/NF-κB signaling attenuates M1 macrophage polarization and alleviates lipopolysaccharide-induced ALI in mice [11]. Similarly, suppression of the TLR4/NF-κB pathway mitigates silica-induced pulmonary inflammation and fibrosis in rats [12]. Furthermore, NF-κB has been identified as an upstream regulator of NLRP3, where excessive activation of the NLRP3 inflammasome exacerbates inflammatory disease progression [13]. Based on this, targeting the TLR4/NF-κB/NLRP3 axis could modulate macrophage polarization and attenuate LIR-ALI.

Esketamine, the S-enantiomer of ketamine, has proven effective in treating treatment-resistant depression (TRD), particularly for rapid symptom relief and reduction in suicidal ideation [14]. Emerging evidence suggests that esketamine possesses systemic anti-inflammatory properties through suppression of pro-inflammatory cytokines. Esketamine reduces ventilator-induced lung injury in chronic obstructive pulmonary disease models by inhibiting the MAPK/NF-κB pathway [15] and ameliorates sepsis-induced lung injury by downregulating Wnt/β-catenin signaling and inflammatory cytokine expression [16]. However, its potential to modulate macrophage polarization and regulate TLR4/NF-κB/NLRP3 axis activation in LIR-ALI remains unexplored.

This study investigates the protective mechanisms of esketamine in LIR-ALI, focusing on its effects on macrophage polarization and pulmonary injury through the TLR4/NF-κB/NLRP3 axis. The findings offer new insights into the regulatory mechanisms of LIR-ALI and lay the groundwork for developing potential therapeutic interventions.

Methods

Experimental Animals and Limb Ischemia-Reperfusion-Induced Acute Lung Injury (LIR-ALI) Model

Eight-week-old male and female Sprague-Dawley (SD) rats, sourced from Guangdong Medical Laboratory Animal Center, were housed in a specific pathogen-free (SPF) environment with controlled conditions (temperature: 22 $\pm$ 2 °C; humidity: 50 $\pm$ 10%; 12-hour light/dark cycle), and provided ad libitum access to chow and water. Rats were randomly assigned to one of three treatment groups (n = 6 per group): (i) Sham (sham operation), (ii) LIR-ALI (LIR-ALI model induction), and (iii) Esketamine (esketamine administration, 230619BL, Jiangsu Hengrui Pharmaceutical Co., Ltd., China). Anesthesia was induced via intraperitoneal injection of propofol (10 mg/kg, Merck, Y0000016). Ventilation parameters were set as follows: tidal volume 6 mL/kg, respiratory rate 80 breaths/min, fraction of inspired oxygen (FiO_2) 0.5, and inspiratory/expiratory (I:E) ratio of 1:1. Mechanical ventilation was maintained during the surgical procedure and throughout the 2-hour ischemia period. Rats were positioned supine on a heating pad to maintain rectal temperature between 37–38 °C. Bilateral groin incisions were made to expose the femoral arteries. In the LIR-ALI and Esketamine groups, bilateral femoral arteries were clamped with atraumatic vascular clips, and tourniquets were applied to the upper thighs to induce limb ischemia. After 2 hours of ischemia, clips and tourniquets were removed to initiate reperfusion. The LIR-ALI group received an intraperitoneal injection of an equal volume of saline 5 minutes before reperfusion, while the Esketamine group was administered 1.6 mg/kg esketamine dissolved in saline via intraperitoneal injection 5 minutes before reperfusion. The Sham group underwent identical anesthesia and surgical procedures (groin incision, femoral artery exposure, and thigh manipulation) without vascular clamping or tourniquet application, and received saline at the corresponding time points. Peripheral blood was collected 12 hours post-reperfusion, and serum was obtained by centrifugation. Bronchoalveolar lavage fluid (BALF) and lung tissue samples were also collected 12 hours after reperfusion. All animal experiments were approved by the Animal Ethics Committee of General Hospital of Ningxia Medical University (KYLL-2022-0531) and conducted in strict adherence to relevant ethical guidelines. At the end of the study, rats were euthanized through intraperitoneal injection of a pentobarbital sodium overdose (100 mg/kg, P3761, Sigma).

Cell Culture and Treatment

Both cell lines were recently authenticated using Short Tandem Repeat (STR) profiling and tested negative for mycoplasma contamination. This study employed the human monocytic cell line THP-1 and the human bronchial ep-

ithelial cell line BEAS-2B, both originally obtained from the Chinese Academy of Sciences Cell Bank (Shanghai, China). The culture medium for both cell lines consisted of DMEM/F12 (Gibco, 11320033, Waltham, MA, USA) supplemented with 10% fetal bovine serum (FBS, Gibco, 26140079, Waltham, MA, USA) and 1% penicillin-streptomycin solution (Beyotime, Cat. No. C0222, Shanghai, China), resulting in final concentrations of 100 U/mL penicillin and 100 µg/mL streptomycin. Cells were maintained at 37 °C in a 5% CO_2 humidified incubator, with medium changes performed regularly.

To induce macrophage differentiation, THP-1 cells were treated with 100 ng/mL phorbol 12-myristate 13-acetate (PMA, Beyotime, S1819, Shanghai, China) for 48 hours, promoting differentiation into adherent macrophages. To determine the optimal concentration of esketamine, differentiated THP-1 macrophages were pretreated with various concentrations of esketamine (0, 10, 50, 100, 200 µM) (Jiangsu Hengrui Pharmaceuticals Co., Ltd., 230619BL, Jiangsu, China) for 24 hours. The medium was then replaced with DMEM/F12 containing 10% heat-inactivated serum from LIR-ALI rats for an additional 24 hours of culture. The Control group was maintained in medium containing 10% heat-inactivated serum from Sham-operated rats.

Coculture Experiment

A coculture system was established using Transwell inserts (pore size: 0.4 µm, Beyotime, FTW001, Shanghai, China). Differentiated THP-1 macrophages were seeded in the upper chamber at a density of 1×10^6 cells/mL. BEAS-2B cells were cultured in the lower chamber. Once appropriate confluence was reached, Transwell inserts were carefully placed into the lower chambers containing BEAS-2B cells. The coculture was maintained for 24 hours before proceeding with subsequent assays.

H&E Staining

Lung tissue specimens were processed following fixation in 4% paraformaldehyde. Tissues were dehydrated through an ethanol gradient, cleared in xylene, and embedded in paraffin. Serial sections (4 µm thick) were prepared using a KD2258 microtome (Leica, Wetzlar, Germany). Sections were deparaffinized in xylene, rehydrated through a descending ethanol gradient (100% to 75%), and stained with hematoxylin and eosin (ServiceBio, G1076, Wuhan, China). After staining, sections were dehydrated through an ascending ethanol series, cleared with xylene, and mounted using neutral balsam. Pathological changes in the lung tissues were evaluated under an optical microscope.

CCK-8 Assay

Cell viability of BEAS-2B cells across treatment groups was assessed using the Cell Counting Kit-8 (CCK-8) assay. Following the manufacturer's instructions, 10 µL of CCK-8 reagent was added to each well, and the plates were incubated for 2 hours at 37 °C in a 5% CO_2 incubator. The optical density at 450 nm was measured using a Bio-Rad 680 microplate reader (Bio-Rad, Hercules, CA, USA).

ELISA Assay

Inflammatory mediator concentrations and oxidative stress parameters were measured using ELISA. The following markers were analyzed: IL-6 (Solarbio, SEKR-0005, Beijing, China), IL-1β (Solarbio, SEKR-0002, Beijing, China), TNF-α (Solarbio, SEKR-0009, Beijing, China), IL-10 (BOSTER, EK0416, Wuhan, China), superoxide dismutase (SOD) (Solarbio, BC5165, Beijing, China), and malondialdehyde (MDA) (Solarbio, BC0025, Beijing, China). All procedures followed the manufacturer's protocols. Optical density readings at specified wavelengths were recorded using a Bio-Rad 680 microplate reader (Bio-Rad, Hercules, CA, USA).

RT-qPCR Analysis

Total RNA was extracted from both rat lung tissues and cultured cells using TRIzol reagent (Beyotime, R0016, Shanghai, China). cDNA synthesis from 1 µg total RNA was performed using the SuperScript IV First-Strand Synthesis System (Beyotime, D7170, Shanghai, China). Real-time quantitative PCR was carried out with SYBR Green Master Mix (Beyotime, D7260, Shanghai, China) and gene-specific primers on a Bio-Rad CFX96 system (Hercules, CA, USA). Relative mRNA expression of target genes was quantified using the $2^{-\Delta\Delta Ct}$ method, with values normalized to internal reference genes. Primer sequences are provided in Table 1.

Western Blot Analysis

Total protein was extracted from tissues or cells using RIPA lysis buffer (Beyotime, P0013B, Shanghai, China) on ice. Protein concentration was quantified using a BCA protein assay kit (Beyotime, P0012S, Shanghai, China). Equal amounts of protein were separated by 10% SDS-PAGE and transferred to PVDF membranes using wet transfer. The membranes were blocked with 5% skim milk for 1 hour at room temperature. For primary antibody detection, membranes were incubated overnight at 4 °C with primary antibodies: Arg-1 (BOSTER, BM4000,Wuhan,

Table 1. Primer sequences in this study.

Name	Primer sequences	Length (bp)
NOS2 F	AGGGACAAGCCTACCCCTC	168
NOS2 R	CTCATCTCCCGTCAGTTGGT	
ARG-1 F	TGGACAGACTAGGAATTGGCA	102
ARG-1 R	CCAGTCCGTCAACATCAAAACT	
GAPDH F	ACAACTTTGGTATCGTGGAAGG	101
GAPDH R	GCCATCACGCCACAGTTTC	

China), TLR4 (Proteintech, 19811-1-AP, Rosemont, IL, USA), NF-κB (CST, #8242, Danvers, MA, USA), p-NF-κB (Abcam, ab76302, Cambridge, UK), NLRP3 (Abcam, ab263899, Cambridge, UK), and GAPDH (CST, #5174, Danvers, MA, USA) as the internal control. After washing, the membranes were exposed to a horseradish peroxidase (HRP)-conjugated secondary antibody (Cat. No. ab97051, Abcam, Cambridge, UK) for 1 hour at room temperature. Protein bands were detected using an enhanced chemiluminescence (ECL) kit, and Western blot bands were quantified using ImageJ software (version 1.54g, Bethesda, MD, USA).

Flow Cytometry Analysis

Flow cytometric analysis was conducted to assess the macrophage surface markers CD86 and CD206. Cells, when reaching 70–80% confluence, were harvested by centrifugation and digestion, followed by PBS washing. The cells were incubated with primary antibodies against CD86 (Boster, BM4121,Wuhan, China) and CD206 (Abcam, ab64693, Cambridge, UK) on ice for 1 hour. After washing with sorting buffer (PBS containing 2% FBS), the cells were incubated with goat anti-rabbit secondary antibody on ice for 30 minutes. A FACSCalibur™ flow cytometer (BD Biosciences, San Jose, CA, USA) was used for sample analysis, and data processing was performed with FlowJo software (BD, Ashland, OR, USA).

Statistical Analysis

Data were analyzed using GraphPad Prism 10, and results are presented as Mean $\pm$ SD. Comparisons among multiple groups were made using one-way analysis of variance (ANOVA) followed by Tukey's post hoc test. The significance levels were set as follows: $p < 0.05$, $p < 0.01$, $p < 0.001$, and $p < 0.0001$.

Result

Esketamine Attenuated Pulmonary Pathological Damage and Modulated Inflammatory Cytokine Expression in BALF of LIR-ALI Rats

To investigate the protective effects of esketamine on LIR-ALI, a rat model of LIR-ALI was first established. As shown in Fig. 1, histopathological analysis revealed significant lung tissue damage and inflammatory cell infiltration in the LIR-ALI model group (ALI group) compared to the sham-operated group (Sham group). Treatment with esketamine (ESK group) alleviated the extent of lung tissue injury, as evidenced by a reduction in damage relative to the ALI group (Fig. 1A). ELISA data demonstrated that LIR-ALI induction caused a marked increase in the BALF concentrations of pro-inflammatory mediators IL-1β, IL-6, and TNF-α ($p < 0.001$), while a significant reduction in the anti-inflammatory cytokine IL-10 was observed ($p < 0.0001$). Esketamine treatment significantly suppressed the levels of pro-inflammatory cytokines and restored IL-10 concentrations ($p < 0.01$) (Fig. 1B,C). These results suggest that esketamine may mitigate LIR-ALI-induced lung injury by inhibiting the release of pro-inflammatory cytokines and promoting anti-inflammatory cytokine expression.

Esketamine Modulated the Expression of Macrophage Polarization Markers in LIR-ALI Rat Lungs

To further explore the impact of esketamine on macrophage polarization in LIR-ALI rat lungs, the expression levels of M1 and M2 macrophage markers were analyzed using RT-qPCR and Western blot. As shown in Fig. 2, ALI induction significantly increased *Nos2* mRNA and iNOS protein levels, while decreasing *Arg-1* mRNA and Arg-1 protein expression in lung tissues ($p < 0.001$). Esketamine treatment (ESK group) significantly reversed these alterations in iNOS and Arg-1 expression ($p < 0.05$) (Fig. 2A,B). These results demonstrate that esketamine promotes macrophage polarization toward the M2 phenotype in LIR-ALI rat lungs by downregulating the M1 marker iNOS and upregulating the M2 marker Arg-1.

Esketamine Modulated Macrophage Polarization Induced by LIR-ALI Rat Serum In Vitro and Attenuated Epithelial Cell Injury

To investigate esketamine's regulation of macrophage polarization and its protective role in pulmonary epithelial cells at the cellular level, a coculture system of pulmonary epithelial cells and macrophages stimulated by phorbol ester (PMA) and LIR-ALI rat serum (ALI serum) was established. First, the CCK-8 assay was performed to assess the impact of different esketamine concentrations (0, 10, 50, 100, 200 μM) on the viability of PMA-induced THP-1 macrophages. As shown in Fig. 3A,B, esketamine exhibited no significant cytotoxicity within the tested concentration range, except for a slight reduction in cell viability at 200 μM ($p < 0.05$). Next, the effect of esketamine on BEAS-2B cell viability in the coculture system with LIR-ALI serum-stimulated macrophages was examined. As presented in Fig. 3B, 10 μM and 50 μM esketamine significantly enhanced the viability of injured BEAS-2B cells, with 50 μM showing a more pronounced effect ($p < 0.01$). Therefore, 50 μM was selected as the optimal concentration for subsequent experiments (Fig. 3A,B). Further validation confirmed that BEAS-2B cell viability was significantly reduced in the ALI group compared to the Control group ($p < 0.0001$). However, pretreatment of macrophages with 50 μM esketamine significantly reversed the inhibitory effect of LIR-ALI serum on BEAS-2B cell viability ($p < 0.01$) (Fig. 3C). RT-qPCR analysis revealed that ALI serum significantly upregulated the mRNA expression of the M1 marker *NOS2* and downregulated the M2 marker *ARG-1* mRNA in THP-1 macrophages compared to the Control group ($p < 0.001$). Esketamine pretreatment reversed these

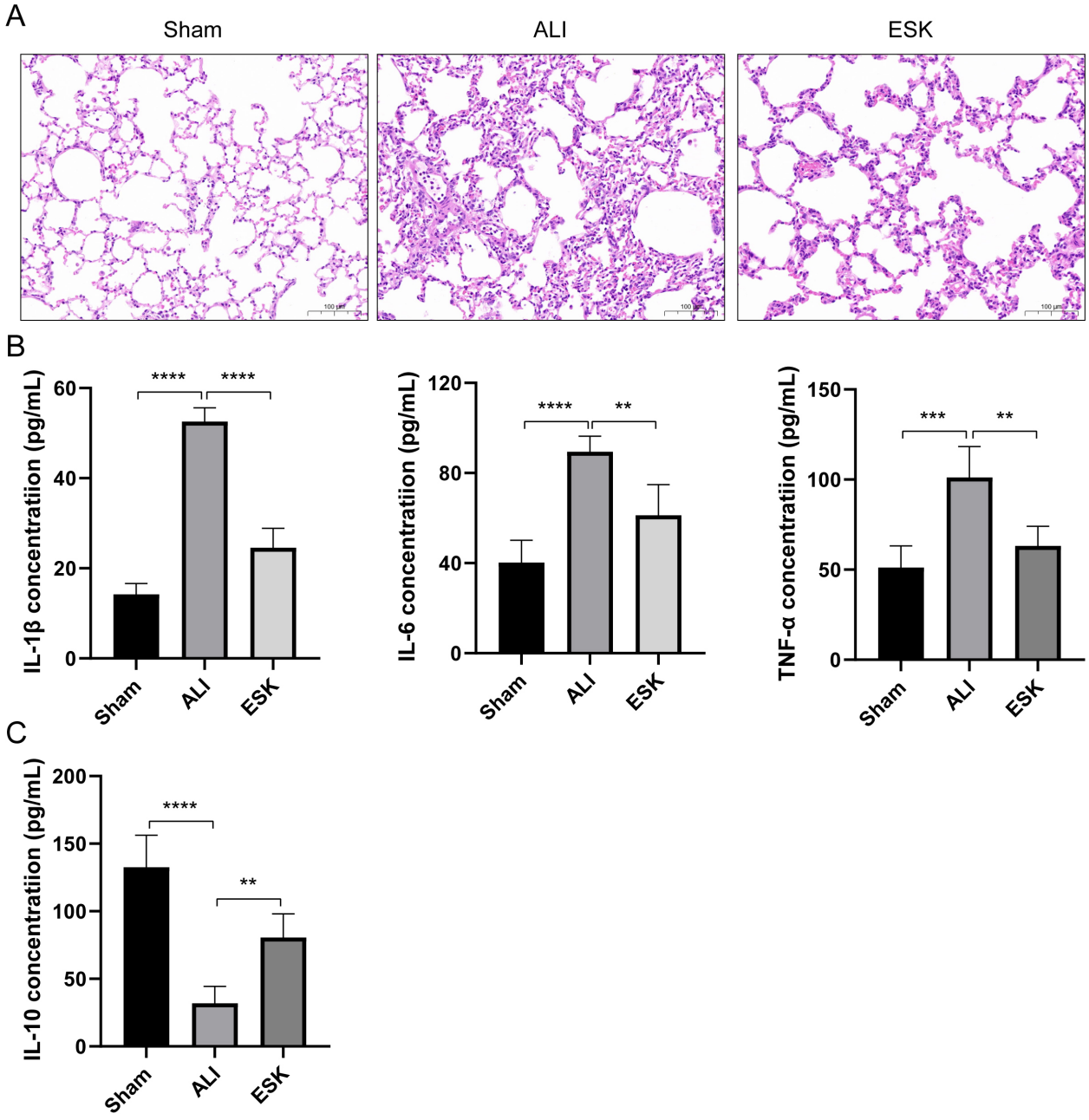

Fig. 1. ESK alleviates LIR-induced pulmonary pathological damage and modulates inflammatory cytokine levels in BALF. (A) H&E staining of lung tissue from Sham, LIR-ALI, and ESK-treated rats. Scale bar = 100 μm. (B) Levels of IL-1β, IL-6, and TNF-α in BALF measured by ELISA. (C) Levels of IL-10 in BALF measured by ELISA. Data are presented as mean ± SD (n = 6 per group). **$p < 0.01$, ***$p < 0.001$, ****$p < 0.0001$. ESK, esketamine; BALF, Bronchoalveolar lavage fluid; ELISA, enzyme-linked immunosorbent assay.

changes, downregulating *NOS2* and upregulating *ARG-1* mRNA expression ($p < 0.001$) (Fig. 3D). Flow cytometry results further confirmed the effect of esketamine on macrophage polarization. As shown in Fig. 3E,F, ALI serum treatment significantly increased the proportion of CD86-positive (M1) macrophages and decreased CD206-positive (M2) cells ($p < 0.0001$). Esketamine pretreatment significantly reduced CD86-positive cells while increasing CD206-positive cells ($p < 0.0001$) (Fig. 3E,F).

Esketamine Attenuated LIR-ALI Serum-Induced Inflammatory Response in BEAS-2B Cells by Suppressing the TLR4/NF-κB/NLRP3 Axis

To further elucidate the molecular mechanism by which esketamine (50 μM) modulates macrophage polarization and protects pulmonary epithelial cells, the expression of key proteins in the TLR4/NF-κB/NLRP3 signaling axis within the coculture system was examined. As shown in Fig. 4, treatment with LIR-ALI serum (ALI group)

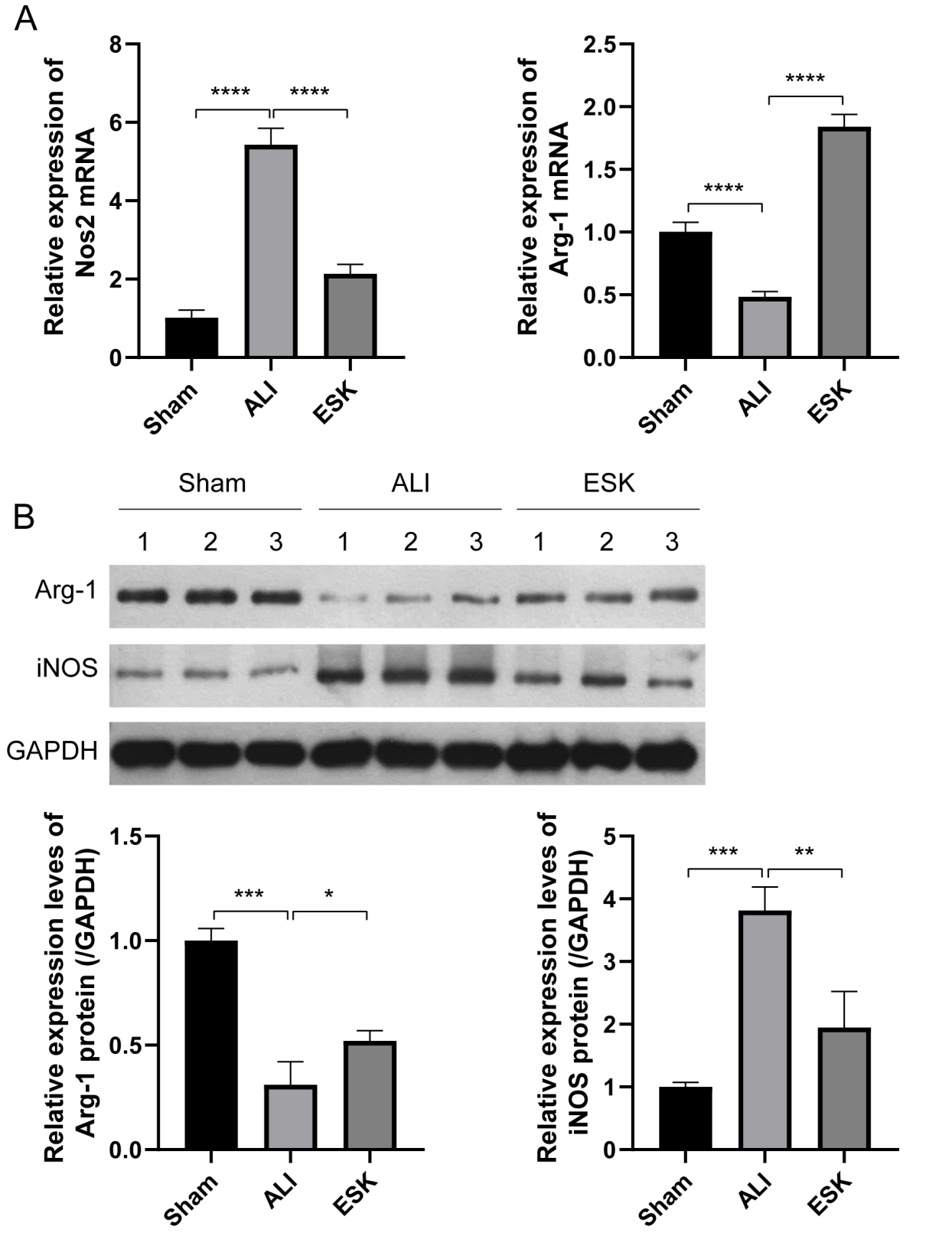

Fig. 2. ESK modulates M1/M2 macrophage polarization markers in LIR-ALI rat lungs. (A) Relative mRNA expression of *Nos2* and *Arg-1* in lung tissues from Sham, LIR-ALI, and ESK-treated rats, measured by RT-qPCR. (B) Representative Western blot bands and quantitative analysis of iNOS and Arg-1 protein expression in lung tissues. GAPDH was used as a loading control. Data are presented as mean ± SD (n = 6 per group). *$p < 0.05$, **$p < 0.01$, ***$p < 0.001$, ****$p < 0.0001$.

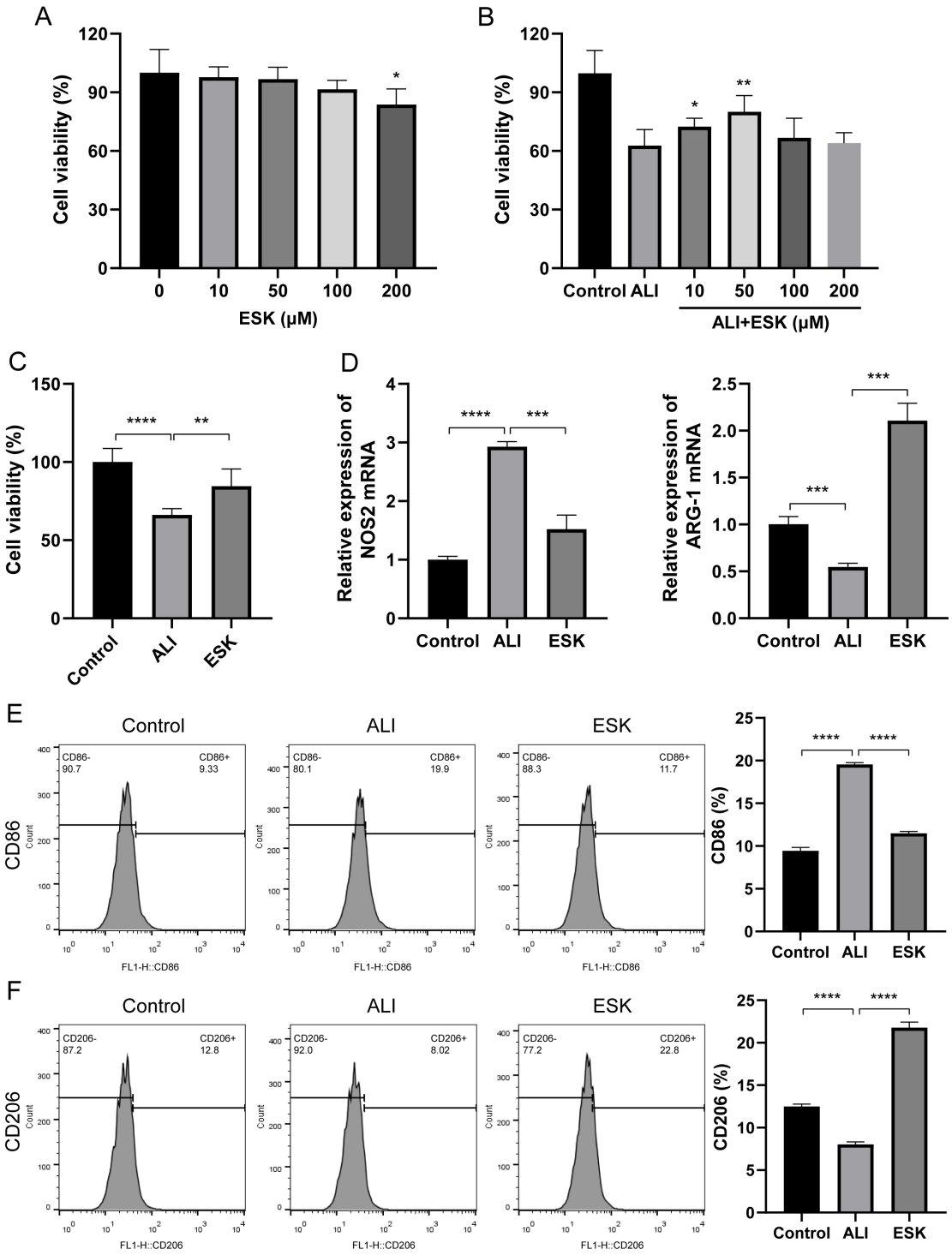

Fig. 3. ESK modulates LIR-ALI serum-induced macrophage polarization and protects BEAS-2B cells *in vitro*. (A) Viability of PMA-differentiated THP-1 macrophages pretreated with ESK (0, 10, 50, 100, 200 μM) for 24 hours, assessed by CCK-8 assay. (B) Viability of BEAS-2B cells co-cultured with LIR-ALI serum-stimulated THP-1 macrophages pretreated with ESK (0, 10, 50, 100, or 200 μM). (C) Viability of BEAS-2B cells co-cultured with THP-1 macrophages: Control, ALI (LIR-ALI serum), and ESK (LIR-ALI serum + 50 μM ESK). (D) Relative mRNA expression of *NOS2* and *ARG-1* in THP-1 macrophages from the indicated treatment groups, determined by RT-qPCR. (E) Representative flow cytometry plots of CD86 expression on THP-1 macrophages. (F) Representative flow cytometry plots of CD206 expression on THP-1 macrophages. Data are presented as mean ± SD from at least three independent experiments. *$p < 0.05$, **$p < 0.01$, ***$p < 0.001$, ****$p < 0.0001$.

markedly increased the secretion of pro-inflammatory factors IL-6 and TNF-α while downregulating the anti-inflammatory cytokine IL-10 in the supernatant of BEAS-2B cells ($p < 0.001$). Esketamine treatment significantly reduced IL-6 and TNF-α levels and restored IL-10 expression ($p < 0.01$) (Fig. 4A). Western blot analysis revealed that LIR-ALI serum treatment significantly elevated the protein expression of TLR4, p-NF-κB, and NLRP3 in macrophages ($p < 0.001$). Notably, esketamine pretreatment significantly suppressed the ALI serum-induced upregulation of TLR4, p-NF-κB, and NLRP3 ($p < 0.01$) (Fig. 4B). These results suggest that esketamine may mitigate LIR-ALI serum-induced inflammatory injury in BEAS-2B pulmonary epithelial cells by inhibiting the TLR4/NF-κB/NLRP3 axis in THP-1 macrophages.

Esketamine Regulated LIR-ALI Serum-Induced Macrophage Polarization Through the TLR4/NF-κB/NLRP3 Axis

To determine whether esketamine's modulation of macrophage polarization depends on the TLR4/NF-κB/NLRP3 axis, the coculture system (pulmonary epithelial cells with PMA and LIR-ALI serum-stimulated macrophages) was treated with the exogenous TLR4 agonist LPS. As shown in Fig. 5A, esketamine treatment significantly reduced the protein expression levels of TLR4, p-NF-κB, and NLRP3 in macrophages ($p < 0.01$), indicating its inhibitory effect on LIR-ALI serum-induced activation of the TLR4/NF-κB/NLRP3 axis. However, LPS treatment reversed this inhibition, significantly increasing the expression of TLR4, p-NF-κB, and NLRP3 compared to the esketamine group ($p < 0.05$). RT-qPCR results demonstrated that esketamine treatment significantly decreased M1 marker *NOS2* mRNA expression while increasing M2 marker *ARG-1* mRNA expression ($p < 0.0001$), promoting M2 polarization. LPS administration counteracted these effects, significantly elevating *NOS2* mRNA and reducing *ARG-1* mRNA levels compared to the ESK group ($p < 0.01$), suggesting a reversion to the M1 phenotype (Fig. 5B). These results indicate that esketamine's regulation of LIR-ALI serum-induced macrophage polarization likely depends on its suppression of the TLR4/NF-κB/NLRP3 axis.

LPS Counteracted the Protective Effects of Esketamine on LIR-ALI Serum-Induced Pulmonary Epithelial Cells

To assess the effect of LPS on esketamine-treated pulmonary epithelial cells exposed to LIR-ALI serum, rescue experiments were conducted, and BEAS-2B cell viability, oxidative stress markers, and inflammatory cytokine levels in the coculture system were evaluated. As shown in Fig. 6, the ALI group exhibited a significant decrease in BEAS-2B cell viability compared to the Control group ($p < 0.0001$), accompanied by a marked increase in malondialdehyde (MDA) levels and a decrease in superoxide dismutase (SOD) activity ($p < 0.0001$). Esketamine treatment significantly enhanced cell viability, reduced MDA levels, and improved SOD activity ($p < 0.0001$). However, LPS administration reversed these beneficial effects ($p < 0.05$) (Fig. 6A–C). ELISA analysis of BEAS-2B cell culture supernatant revealed that, compared to the Control group, the ALI group had significantly elevated levels of pro-inflammatory cytokines (IL-6 and TNF-α) and reduced anti-inflammatory IL-10 levels ($p < 0.0001$). Esketamine treatment significantly lowered IL-6 and TNF-α levels while increasing IL-10 ($p < 0.01$). These effects were similarly reversed by LPS treatment ($p < 0.01$) (Fig. 6D). In summary, esketamine effectively improved cell viability, mitigated oxidative stress, and reduced inflammation in pulmonary epithelial cells exposed to LIR-ALI serum. However, these protective effects were abolished by LPS administration.

Discussion

LIR-ALI, a common complication following vascular surgery or severe trauma, involves acute lung inflammation triggered by limb reperfusion [17]. Current clinical management of ALI primarily relies on lung-protective ventilation and restrictive fluid therapy, supplemented with glucocorticoids, inhaled pulmonary vasodilators, neuromuscular blockers, and extracorporeal membrane oxygenation. However, the prognosis for most patients with ALI remains poor, and no specific therapeutic approach for ALI exists [18,19]. Given its significant impact on patient outcomes and the limitations of current treatments, identifying novel, effective, and safe therapeutic strategies for LIR-ALI is critical.

Esketamine, an analgesic and anesthetic agent, not only exhibits bronchodilatory effects and enhances pulmonary diffusion capacity but also demonstrates anti-inflammatory properties during pulmonary surgery [20]. A clinical study has shown that esketamine improves postoperative respiratory function and reduces pulmonary complications in patients undergoing VATS lobectomy [21]. Through modulation of the ULK1/FUNDC1 signaling pathway, esketamine enhances pulmonary vascular permeability while suppressing inflammation and oxidative stress [22]. Furthermore, combination therapy with esketamine significantly alleviates pain, promotes postoperative recovery, and reduces complication rates, offering valuable insights for postoperative analgesia and complication prevention. For instance, a randomized double-blind controlled trial revealed that esketamine combined with dexmedetomidine substantially reduces postoperative opioid consumption and pain scores while improving recovery quality in major laparoscopic surgeries [23]. In the present study, a rat LIR-ALI model was established to evaluate the protective effects of esketamine. The results demonstrated that

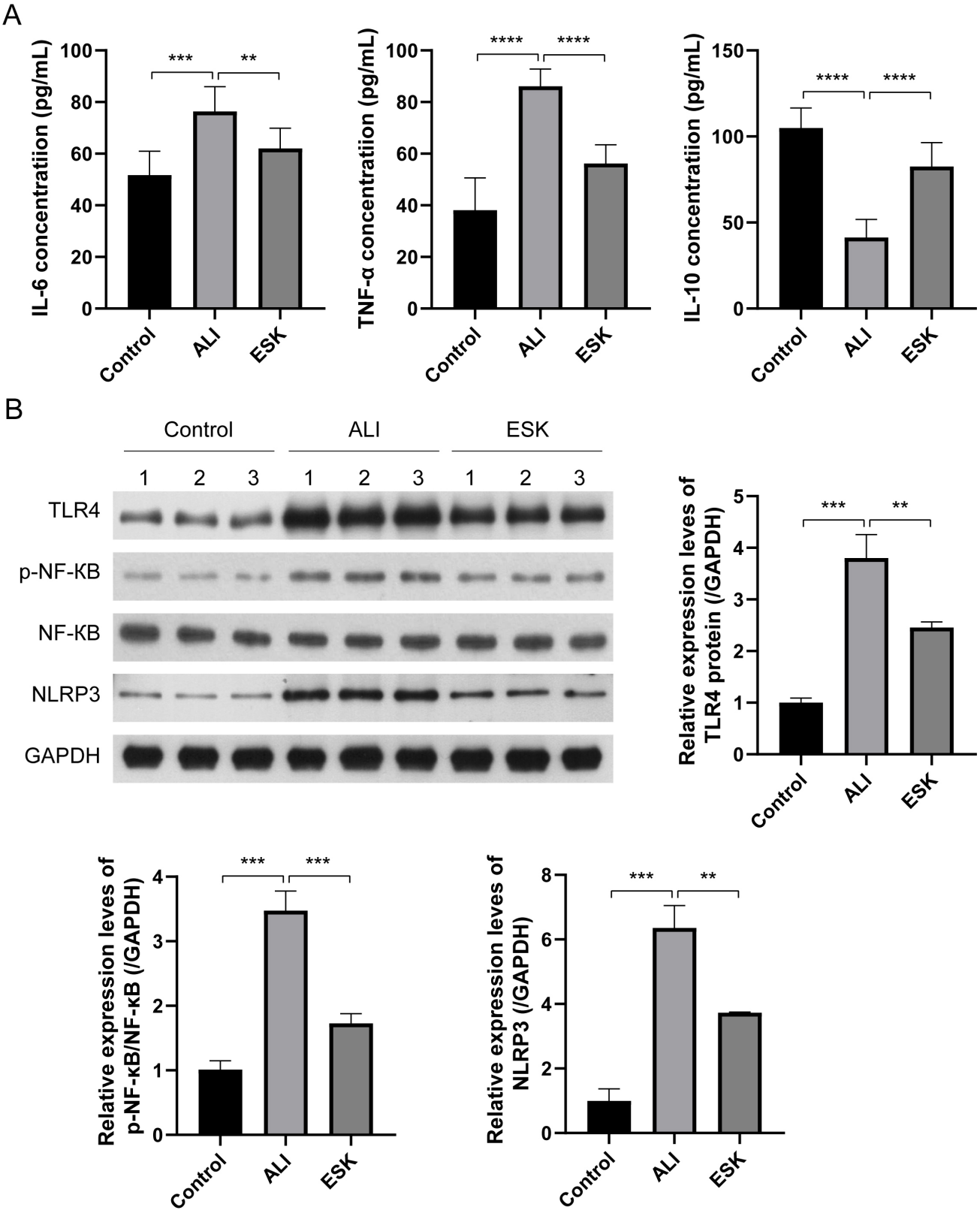

Fig. 4. ESK suppresses the TLR4/NF-κB/NLRP3 axis in macrophages and reduces LIR-ALI serum-induced inflammation in co-cultured BEAS-2B cells. (A) Levels of IL-6, TNF-α, and IL-10 in the supernatant of BEAS-2B cells co-cultured with THP-1 macrophages (Control, ALI, or ESK groups), measured by ELISA. (B) Representative Western blot bands and quantitative analysis of TLR4, p-NF-κB, and NLRP3 protein expression in THP-1 macrophages. GAPDH was used as a loading control. Data are presented as mean $\pm$ SD from at least three independent experiments. $^{**}p < 0.01$, $^{***}p < 0.001$, $^{****}p < 0.0001$.

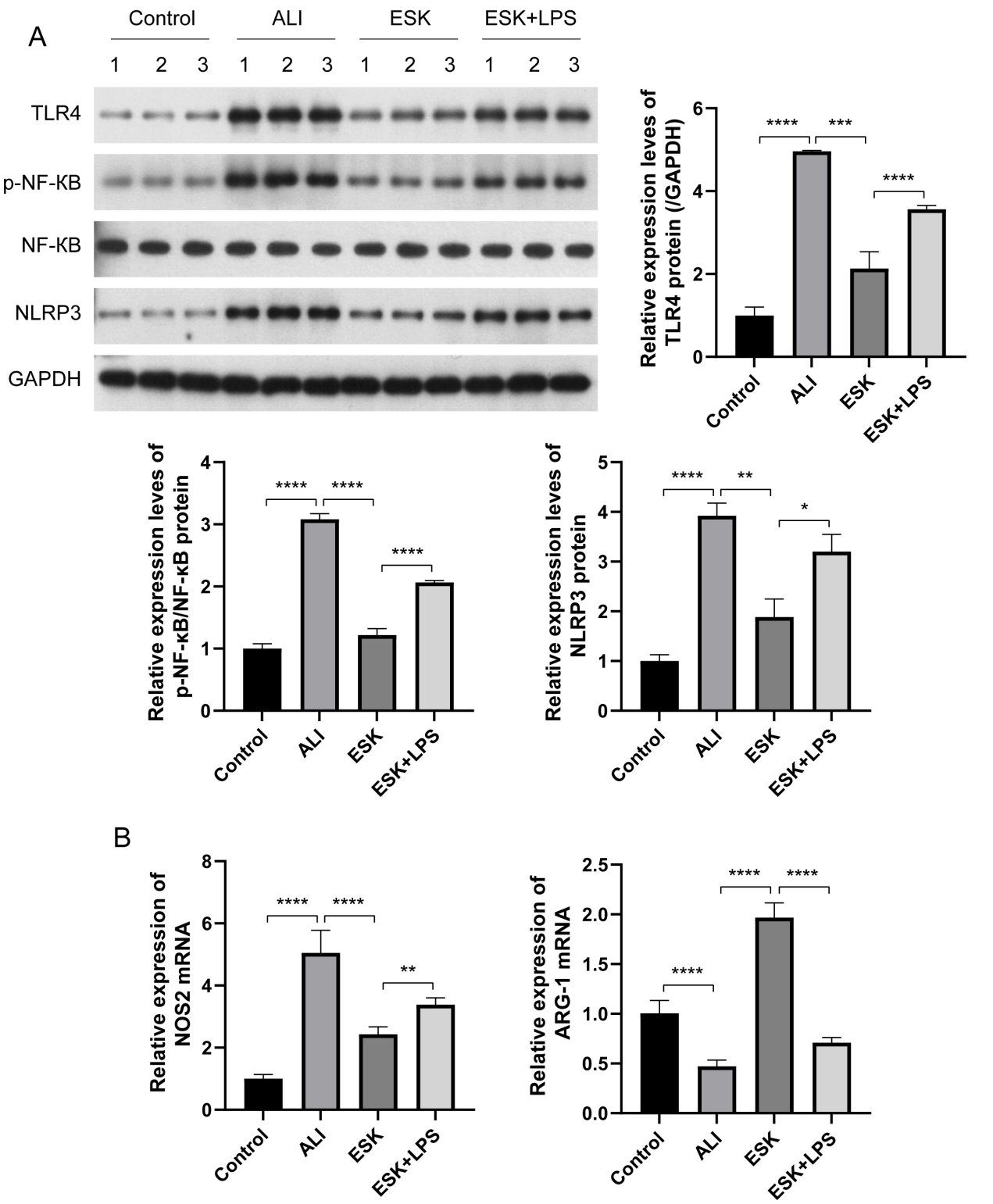

Fig. 5. ESK-mediated macrophage polarization involves the TLR4/NF-κB/NLRP3 axis. THP-1 macrophages were pretreated with ESK (50 μM) and/or LPS before or during stimulation with LIR-ALI serum. (A) Representative Western blot bands and quantitative analysis of TLR4, p-NF-κB, and NLRP3 protein expression in THP-1 macrophages from Control, ALI, ESK, and ESK+LPS groups. GAPDH served as a loading control. (B) Relative mRNA expression of *NOS2* and *ARG-1* in THP-1 macrophages from the indicated treatment groups, determined by RT-qPCR. Data are presented as mean ± SD from at least three independent experiments. *$p < 0.05$, **$p < 0.01$, ***$p < 0.001$, ****$p < 0.0001$.

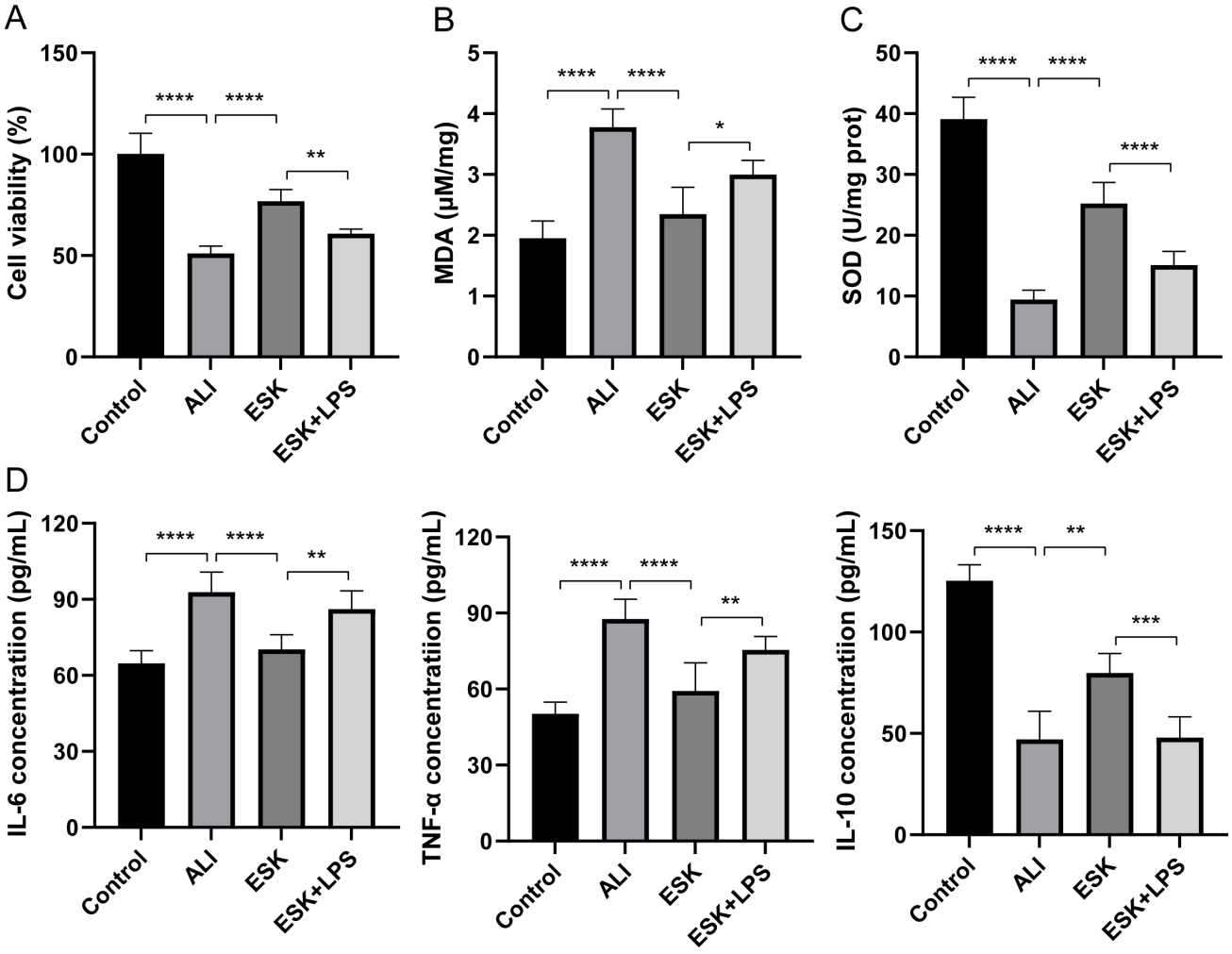

Fig. 6. LPS counteracts the protective effects of ESK on LIR-ALI serum-induced injury in BEAS-2B cells. (A) Viability of BEAS-2B cells assessed by CCK-8 assay. (B) MDA levels in BEAS-2B cells. (C) SOD activity in BEAS-2B cells. (D) Levels of IL-6, TNF-α, and IL-10 in the supernatant of BEAS-2B cells, measured by ELISA. Data are presented as mean $\pm$ SD from at least three independent experiments. *$p < 0.05$, **$p < 0.01$, ***$p < 0.001$, ****$p < 0.0001$. SOD, superoxide dismutase.

esketamine significantly alleviated pathological lung injury and inflammatory cell infiltration in LIR-ALI rats, while reducing pro-inflammatory cytokine levels (IL-1β, IL-6, TNF-α) and increasing anti-inflammatory cytokine (IL-10) levels in BALF. Moreover, esketamine downregulated M1 macrophage markers (iNOS/NOS2) and upregulated M2 macrophage markers (Arg-1). These findings suggest that esketamine may provide critical lung protection in LIR-ALI by promoting macrophage polarization toward the M2 phenotype and modulating inflammatory cytokine secretion.

ALI development is often associated with an imbalance in pulmonary macrophage polarization, where dynamic changes in the M1/M2 ratio directly influence inflammation and disease progression [24]. In inflamed lung tissues, macrophages predominantly adopt an M1 phenotype, secreting pro-inflammatory cytokines that exacerbate ALI progression [24,25]. For instance, inhibiting NF-κB/PPARγ-mediated M1 macrophage polarization has been shown to alleviate CLP-induced lung injury [26]. Similarly, in LPS-induced ALI, blocking M1 polarization effectively reduces pulmonary damage and inflammation in murine models [27]. Consequently, modulating macrophage polarization and infiltration is considered a promising therapeutic strategy for mitigating ALI severity. In our experiments using a macrophage model induced by phorbol ester and LIR-ALI rat serum, esketamine pretreatment significantly decreased M1 marker expression (CD86, NOS2) while increasing M2 markers (CD206, Arg-1). These results suggest that esketamine may alleviate LIR-ALI by restoring the M1/M2 balance. Additionally, the underlying regulatory mechanisms of esketamine in LIR-ALI were investigated.

NLRP3 is a key regulatory molecule in the pathogenesis of ALI. Studies show that both the expression and activation of NLRP3 are significantly increased in lung tissues of patients with ALI, correlating positively with dis-

ease severity [28]. Consequently, targeting NLRP3 has emerged as a promising therapeutic strategy for ALI. Notably, NLRP3 interacts extensively with the TLR4/NF-κB signaling pathway. Activation of TLR4 induces phosphorylation and nuclear translocation of NF-κB, which regulates pro-inflammatory gene expression associated with M1 macrophages and contributes to ALI progression [29, 30]. For example, endothelial-derived SPARLC1 exacerbates lung injury by activating the TLR4/NF-κB pathway, driving the conversion of M2 reparative macrophages into M1 pro-inflammatory phenotypes [31]. In sepsis-induced lung injury, inhibition of LPS/TLR4-mediated NF-κB and IRF signaling effectively attenuates macrophage inflammatory responses and blocks M1 polarization [32, 33]. Moreover, NF-κB serves as a "priming signal" for NLRP3 inflammasome activation, amplifying inflammatory signaling and tissue damage. For instance, suppressing the TLR4/NF-κB/NLRP3 cascade can promote the conversion of M1 macrophages to an M2 phenotype, thereby alleviating LIR-induced lung injury [34]. In our experiments using a macrophage-BEAS-2B coculture system, esketamine attenuated LIR-ALI serum-induced inflammation and oxidative stress in BEAS-2B cells by inhibiting the TLR4/NF-κB/NLRP3 axis in macrophages while promoting M2 macrophage polarization. Notably, LPS treatment, as an exogenous TLR4 agonist, reactivated the TLR4/NF-κB/NLRP3 pathway, resulting in a shift in macrophage polarization and modulating both inflammatory cytokine secretion and oxidative stress levels in pulmonary epithelial cells. These results suggest that esketamine mitigates ALI-associated inflammation and promotes M2 macrophage polarization through inhibition of the TLR4/NF-κB/NLRP3 axis.

Notably, our *in vitro* experiments utilized a cross-species design, with human cell lines stimulated by rat serum. Although the TLR4/NF-κB pathway is highly conserved across species, potential variations in cytokine-receptor affinity between rats and humans may introduce unforeseen variables. However, the consistency observed between our *in vivo* and *in vitro* findings supports the validity of this model for translational research.

Conclusion

In conclusion, this study demonstrates that esketamine plays a protective role in LIR-ALI. Using both rat LIR-ALI models and a serum-based cell coculture system, this study showed that esketamine significantly drives M2 macrophage polarization while suppressing M1 markers via the TLR4/NF-κB/NLRP3 axis. This mechanism effectively mitigated pathological lung damage, reduced inflammatory cell infiltration in LIR-ALI rats, and improved inflammatory responses and oxidative stress in pulmonary epithelial cells. These findings not only enhance our understanding of macrophage polarization imbalance in LIR-ALI pathogenesis but also provide new experimental evidence and molecular targets for the clinical application of esketamine. The results highlight the clinical translational potential of esketamine, offering novel insights for developing effective interventions against LIR-ALI.

Availability of Data and Materials

All data are available from the corresponding author upon reasonable request.

Author Contributions

MW and QM designed the study. MW, JC, WW and PW acquired the data and analysis and perform the experiment. WW and PW analyzed and interpreted the data. HW processed the data and generated the figures. MW and JC drafted the manuscript. WW, PW, HW and QM critically revised the manuscript. All authors read and approved the manuscript. All authors give final approval of the version to be published. All authors have participated sufficiently in the work to take public responsibility for appropriate portions of the content and agreed to be accountable for all aspects of the work in ensuring that questions related to its accuracy or integrity.

Ethics Approval and Consent to Participate

The reported experiments are in accordance with the standards set forth in "Guide for the Care and Use of Laboratory Animals". This study adheres to internationally accepted standards for animal research, following the 3Rs principle. All animal experiments were approved by the Animal Ethics Committee of General Hospital of Ningxia Medical University (KYLL-2022-0531).

Acknowledgment

Not applicable.

Funding

This study was supported by Natural Science Foundation of Ningxia (No.2023AAC03583, Meng Wang) and Natural Science Foundation of Ningxia (No.2023AAC03630, Qian Ma).

Conflict of Interest

The authors declare no conflict of interest.

References

[1] Lu K, Ling M, Rao M, Huang H, Liang S, Wei Y, *et al*. Identification of Hub Genes for Dexmedetomidine Alleviation of Limb Ischemia-Reperfusion-Induced Lung Injury in Rats by Tran-

scriptomic. Journal of Inflammation Research. 2025; 18: 5427–5445. https://doi.org/10.2147/JIR.S512536.

[2] Wen H, Zhang H, Wang W, Li Y. Tetrahydropalmatine protects against acute lung injury induced by limb ischemia/reperfusion through restoring PI3K/AKT/mTOR-mediated autophagy in rats. Pulmonary Pharmacology & Therapeutics. 2020; 64: 101947. https://doi.org/10.1016/j.pupt.2020.101947.

[3] Zhang S, Zhao X, Xue Y, Wang X, Chen XL. Advances in nanomaterial-targeted treatment of acute lung injury after burns. Journal of Nanobiotechnology. 2024; 22: 342. https://doi.org/10.1186/s12951-024-02615-0.

[4] Rodríguez-Morales P, Franklin RA. Macrophage phenotypes and functions: resolving inflammation and restoring homeostasis. Trends in Immunology. 2023; 44: 986–998. https://doi.org/10.1016/j.it.2023.10.004.

[5] Wang C, Ma C, Gong L, Guo Y, Fu K, Zhang Y, *et al*. Macrophage Polarization and Its Role in Liver Disease. Frontiers in Immunology. 2021; 12: 803037. https://doi.org/10.3389/fimmu.2021.803037.

[6] Li J, Ma W, Tang Z, Li Y, Zheng R, Xie Y, *et al*. Macrophage-driven pathogenesis in acute lung injury/acute respiratory disease syndrome: Harnessing natural products for therapeutic interventions (Review). Molecular Medicine Reports. 2025; 31: 16. https://doi.org/10.3892/mmr.2024.13381.

[7] Yang W, Tao K, Zhang P, Chen X, Sun X, Li R. Maresin 1 protects against lipopolysaccharide/d-galactosamine-induced acute liver injury by inhibiting macrophage pyroptosis and inflammatory response. Biochemical Pharmacology. 2022; 195: 114863. https://doi.org/10.1016/j.bcp.2021.114863.

[8] Zou R, Wang MH, Chen Y, Fan X, Yang B, Du J, *et al*. Hydrogen-Rich Saline Attenuates Acute Lung Injury Induced by Limb Ischemia/Reperfusion via Down-Regulating Chemerin and NLRP3 in Rats. Shock (Augusta, Ga.). 2019; 52: 134–141. https://doi.org/10.1097/SHK.0000000000001194.

[9] Zusso M, Lunardi V, Franceschini D, Pagetta A, Lo R, Stifani S, *et al*. Ciprofloxacin and levofloxacin attenuate microglia inflammatory response via TLR4/NF-kB pathway. Journal of Neuroinflammation. 2019; 16: 148. https://doi.org/10.1186/s12974-019-1538-9.

[10] Zhao H, Chen Z, Xie LJ, Liu GF. Suppression of TLR4/NF-κB Signaling Pathway Improves Cerebral Ischemia-Reperfusion Injury in Rats. Molecular Neurobiology. 2018; 55: 4311–4319. https://doi.org/10.1007/s12035-017-0552-0.

[11] Ren AQ, Wang HJ, Zhu HY, Ye G, Li K, Chen DF, *et al*. Glycoproteins From *Rabdosia japonica* var. *glaucocalyx* Regulate Macrophage Polarization and Alleviate Lipopolysaccharide-Induced Acute Lung Injury in Mice *via* TLR4/NF-κB Pathway. Frontiers in Pharmacology. 2021; 12: 693298. https://doi.org/10.3389/fphar.2021.693298.

[12] Zhang Y, Liu F, Jia Q, Zheng L, Tang Q, Sai L, *et al*. Baicalin alleviates silica-induced lung inflammation and fibrosis by inhibiting TLR4/NF-?B pathway in rats. Physiological Research. 2023; 72: 221–233. https://doi.org/10.33549/physiolres.934978.

[13] Afonina IS, Zhong Z, Karin M, Beyaert R. Limiting inflammation-the negative regulation of NF-κB and the NLRP3 inflammasome. Nature Immunology. 2017; 18: 861–869. https://doi.org/10.1038/ni.3772.

[14] Salahudeen MS, Wright CM, Peterson GM. Esketamine: new hope for the treatment of treatment-resistant depression? A narrative review. Therapeutic Advances in Drug Safety. 2020; 11: 2042098620937899. https://doi.org/10.1177/2042098620937899.

[15] Cai SY, Liu A, Xie WX, Zhang XQ, Su B, Mao Y, *et al*. Esketamine mitigates mechanical ventilation-induced lung injury in chronic obstructive pulmonary disease rats via inhibition of the MAPK/NF-κB signaling pathway and reduction of oxidative stress. International Immunopharmacology. 2024; 139: 112725. https://doi.org/10.1016/j.intimp.2024.112725.

[16] Xie B, Wang M, Zhang X, Zhang Y, Qi H, Liu H, *et al*. Gut-derived memory γδ T17 cells exacerbate sepsis-induced acute lung injury in mice. Nature Communications. 2024; 15: 6737. https://doi.org/10.1038/s41467-024-51209-9.

[17] Liu L, Yang C, Qiu T, Shen X, Liu B, Qi X, *et al*. Hydrogen alleviates acute lung injury induced by limb ischaemia/reperfusion in mice. Life Sciences. 2021; 279: 119659. https://doi.org/10.1016/j.lfs.2021.119659.

[18] Lewis SR, Pritchard MW, Thomas CM, Smith AF. Pharmacological agents for adults with acute respiratory distress syndrome. The Cochrane Database of Systematic Reviews. 2019; 7: CD004477. https://doi.org/10.1002/14651858.CD004477.pub3.

[19] Nanchal RS, Truwit JD. Recent advances in understanding and treating acute respiratory distress syndrome. F1000Research. 2018; 7: F1000 Faculty Rev–1322. https://doi.org/10.12688/f1000research.15493.1.

[20] Lei Y, Liu H, Xia F, Gan S, Wang Y, Huo W, *et al*. Effects of Esketamine on Acute and Chronic Pain After Thoracoscopy Pulmonary Surgery Under General Anesthesia: A Multicenter-Prospective, Randomized, Double-Blind, and Controlled Trial. Frontiers in Medicine. 2021; 8: 693594. https://doi.org/10.3389/fmed.2021.693594.

[21] Fu M, Xu R, Chen G, Zheng X, Shu B, Huang H, *et al*. Postoperative esketamine improves ventilation after video-assisted thoracoscopic lung resection: A double-blinded randomized controlled trial. Heliyon. 2024; 10: e25100. https://doi.org/10.1016/j.heliyon.2024.e25100.

[22] Ding M, Pei P, Liu W, Cao Y, Weng Y, Yu W. Esketamine Regulates Mitophagy through ULK1/FUNDC1 Signaling Pathway to Improve LPS-induced Acute Respiratory Distress Syndrome. Current Pharmaceutical Design. 2025; 31: 2774–2782. https://doi.org/10.2174/0113816128361112250221065359.

[23] Wang W, Chen Y, Li G, Chen Y, Wu J, Shi Y, *et al*. The Opioid-Sparing Effects of Intraoperative Esketamine Combined with Dexmedetomidine During Laparoscopic Major Abdominal Surgery: A Randomized Controlled Double-Blind Trial. Drug Design, Development and Therapy. 2025; 19: 1971–1981. https://doi.org/10.2147/DDDT.S480700.

[24] Pérez S, Rius-Pérez S. Macrophage Polarization and Reprogramming in Acute Inflammation: A Redox Perspective. Antioxidants (Basel, Switzerland). 2022; 11: 1394. https://doi.org/10.3390/antiox11071394.

[25] Lu HL, Huang XY, Luo YF, Tan WP, Chen PF, Guo YB. Activation of M1 macrophages plays a critical role in the initiation of acute lung injury. Bioscience Reports. 2018; 38: BSR20171555. https://doi.org/10.1042/BSR20171555.

[26] Luo J, Wang J, Zhang J, Sang A, Ye X, Cheng Z, *et al*. Nrf2 Deficiency Exacerbated CLP-Induced Pulmonary Injury and Inflammation through Autophagy- and NF-κB/PPARγ-Mediated Macrophage Polarization. Cells. 2022; 11: 3927. https://doi.org/10.3390/cells11233927.

[27] Li B, Xia C, He W, Liu J, Duan R, Ji Z, *et al*. The Thyroid Hormone Analog GC-1 Mitigates Acute Lung Injury by Inhibiting M1 Macrophage Polarization. Advanced Science (Weinheim, Baden-Wurttemberg, Germany). 2024; 11: e2401931. https://doi.org/10.1002/advs.202401931.

[28] Gu W, Zeng Q, Wang X, Jasem H, Ma L. Acute Lung Injury and the NLRP3 Inflammasome. Journal of Inflammation Research. 2024; 17: 3801–3813. https://doi.org/10.2147/JIR.S464838.

[29] Zhang C, Yang Y. Targeting toll-like receptor 4 (TLR4) and the NLRP3 inflammasome: Novel and emerging therapeutic targets for hyperuricaemia nephropathy. Biomolecules & Biomedicine. 2023; 24: 688–697. https://doi.org/10.17305/bb.2023.9838.

[30] Fu Y, Gong T, Loughran PA, Li Y, Billiar TR, Liu Y, *et al*. Roles

of TLR4 in macrophage immunity and macrophage-pulmonary vascular/lymphatic endothelial cell interactions in sepsis. Communications Biology. 2025; 8: 469. https://doi.org/10.1038/s42003-025-07921-3.

[31] Zhao G, Gentile ME, Xue L, Cosgriff CV, Weiner AI, Adams-Tzivelekidis S, *et al*. Vascular endothelial-derived SPARCL1 exacerbates viral pneumonia through pro-inflammatory macrophage activation. Nature Communications. 2024; 15: 4235. https://doi.org/10.1038/s41467-024-48589-3.

[32] Li Y, Ai S, Li Y, Ye W, Li R, Xu X, *et al*. The role of natural products targeting macrophage polarization in sepsis-induced lung injury. Chinese Medicine. 2025; 20: 19. https://doi.org/10.1186/s13020-025-01067-4.

[33] Zhang X, Ling C, Xiong Z, Gong T, Luo S, Liu X, *et al*. Desuccinylation of TBK1 by SIRT5 regulates inflammatory response of macrophages in sepsis. Cell Reports. 2024; 43: 115060. https://doi.org/10.1016/j.celrep.2024.115060.

[34] Wen H, Lu D, Chen H, Zhu Y, Xie Q, Zhang Z, *et al*. Tetrahydropalmatine induces the polarization of M1 macrophages to M2 to relieve limb ischemia-reperfusion-induced lung injury via inhibiting the TLR4/NF-κB/NLRP3 signaling pathway. Drug Development Research. 2022; 83: 1362–1372. https://doi.org/10.1002/ddr.21965.